NASA Technical Memorandum 104566, Vol. 2

SeaWiFS Technical Report Series

Stanford B. Hooker and
Elaine R. Firestone, Editors

Volume 2, Analysis of Orbit Selection for SeaWiFS: Ascending vs. Descending Node

Watson W. Gregg

September 1992

NASA Technical Memorandum 104566, Vol. 2

SeaWiFS Technical Report Series

Stanford B. Hooker, Editor
NASA Goddard Space Flight Center
Greenbelt, Maryland

Elaine R. Firestone, Technical Editor
General Sciences Corporation
Laurel, Maryland

Volume 2, Analysis of Orbit Selection for SeaWiFS: Ascending vs. Descending Node

Watson W. Gregg
NASA Goddard Space Flight Center
Greenbelt, Maryland

National Aeronautics and
Space Administration

Goddard Space Flight Center
Greenbelt, Maryland 20771

1992

Author's Note

This Technical Memorandum is a re-release of NASA TM 104546, originally published in September 1991, under the same title. It is being re-released here to provide completeness for the SeaWiFS Technical Report Series. However, some aspects of the SeaWiFS mission have changed since the original printing. The Pegasus will not be carried aloft by a B-52, but rather by a refitted Lockheed L-1011. A daytime launch, however, with its consequent decending node orbit, is still the preferred option due to increased visibility at launch time. The remainder of this TM analyzes the consequences of descending node orbits in relation to ascending node orbits, and remains an applicable analysis.

Greenbelt, Maryland
August 1992

—W. W. G.

Abstract

Due to range safety considerations, the Sea-viewing Wide Field-of-view Sensor (SeaWiFS) ocean color instrument may be required to be launched into a near-noon descending node, as opposed to the ascending node used by the predecessor sensor, the Coastal Zone Color Scanner (CZCS). The relative importance of ascending versus descending near-noon orbits was assessed here to determine if descending node will meet the scientific requirements of SeaWiFS. Analyses focused on ground coverage, local times of coverage, solar and viewing geometries (zenith and azimuth angles), and sun glint. Differences were found in the areas covered by individual orbits, but were not important when taken over a 16 day repeat time. Local time of coverage was also different: for ascending node orbits the Northern Hemisphere was observed in the morning and the Southern Hemisphere in the afternoon, while for descending node orbits the Northern Hemisphere was observed in the afternoon and the Southern in the morning. There were substantial differences in solar azimuth and spacecraft azimuth angles both at equinox and at the Northern Hemisphere summer solstice. Negligible differences in solar and spacecraft zenith angles, relative azimuth angles, and sun glint were obtained at the equinox. However, large differences were found in solar zenith angles, relative azimuths and sun glint for the solstice. These differences appeared to compensate across the scan, however, an increase in sun glint in descending node over that in ascending node on the western part of the scan was compensated by a decrease on the eastern part of the scan. Thus, no advantage or disadvantage could be conferred upon either ascending node or descending node for noon orbits. Analyses were also performed for ascending and descending node orbits that deviated from a noon equator crossing time. For ascending node, afternoon orbits produced the lowest mean solar zenith angles in the Northern Hemisphere; and morning orbits produced the lowest angles for the Southern Hemisphere. For descending node, morning orbits produced the lowest mean solar zenith angles for the Northern Hemisphere; afternoon orbits produced the lowest angles for the Southern Hemisphere.

1. INTRODUCTION

The purpose of this report is to investigate the importance of ascending versus descending node orbits for the Sea-viewing Wide Field-of-view Sensor (SeaWiFS), due for launch in the latter part of August, 1993. SeaWiFS is designed to make global observations of ocean color. The sensor will be carried by the spacecraft SeaStar, which is in turn carried by the launch vehicle, Orbital Sciences Corporation's Pegasus. Unlike traditional launch vehicles, the Pegasus must be carried to high altitude before launch, usually by a NASA B-52 from Edwards Air Force Base in California.

The issue of ascending versus descending node orbits arises due to launch considerations for the Pegasus vehicle. Specifically, range safety requires a launch to the south from the western United States. A noon ascending node orbit requires a night launch of the Pegasus from Edwards Air Force Base in California. The NASA B-52 carrier vehicle is poorly equipped for night launches and chase planes are less effective at night. A noon descending node orbit may be launched during the daytime. Thus discussion has turned to the scientific need for an ascending node orbit and whether a descending node orbit might accomplish the scientific purposes of SeaWiFS. The predecessor sensor to SeaWiFS, the Coastal Zone Color Scanner (CZCS), was in a noon ascending node orbit.

The analyses here attempt to clarify this issue by focusing on solar geometry (solar zenith and azimuth), viewing geometry (spacecraft zenith and azimuth), and the derived parameters relative azimuth (sun-sensor angle) and sun glint (specular reflection by the sun off the ocean surface). Sun glint is a major contaminant of ocean observations and is calculable from the solar and viewing geometries. Solar zenith is defined as the angle from local nadir to the sun and spacecraft zenith is the angle to the spacecraft. The zenith angles determine the path length of irradiance and radiance through the atmosphere and the effectiveness of the atmospheric correction algorithm. Solar azimuth is defined as the angle from True North to the sub-solar point, measured relative to the pixel. Spacecraft azimuth is defined similarly with respect to the sub-satellite point. These parameters are most important with respect to sun glint, but also determine the contribution of scattering to the total signal received by the sensor.

2. METHODS

Computations were performed using orbital dynamics and Earth location code derived from Wilson et al. (1981). The code was modified to correct the computation of spacecraft azimuth angle and several quadrant ambiguities in the computation of azimuth, longitude and latitude. Most of these corrections were important only near the poles and the dateline. The SeaStar orbit is assumed circular and coverage is calculated for global area coverage (GAC) for which the scan period is 0.667 sec and the swath width is $\pm 45°$. Other orbit and sensor parameters are described in Table 1.

Table 1. SeaStar orbital simulation parameters and SeaWiFS instrument characteristics.

SeaStar Orbital Parameters	
Altitude	705 km
Orbital Repeat Time	16 days (233 orbits)
Period	98.9 minutes
Inclination	98.25°
Equatorial Crossing Time	Noon (local time)
SeaWiFS Instrument Characteristics (GAC)	
Scan Width	$\pm 45°$
Ground IFOV at nadir	1.13 km
Pixels Along Scan	981
Scan Period	0.667 seconds
Tilt	$\pm 20°$
Ground Coverage along Scan	1487 km
Successive Orbit Equatorial Crossing Longitude	$-24.721°$

Computations were performed for Julian Day 80, the vernal equinox, and Julian Day 182, the Northern Hemisphere summer solstice. In both cases the sensor is assumed to scan from west to east. The tilt strategy for both ascending and descending nodes is designed to minimize sun glint. Generally, the sensor tilts away from the sub-solar point (defined by the solar declination). The strategy used here is shown in Table 2.

Table 2. Tilt strategy used for computation of importance of ascending or descending node orbits for SeaWiFS. Fore is defined as along the direction of motion of the spacecraft, aft is backward to the direction of motion, and Ψ is the solar declination latitude.

Sub-satellite Point	Tilt
>60° south of Ψ	0° (nadir)
>60° north of Ψ	0° (nadir)
60° south of Ψ to Ψ	20° aft for ascending 20° fore for descending
60° north of Ψ to Ψ	20° fore for ascending 20° aft for descending

Sun glint was computed from these geometric parameters using the Cox and Munk (1954) theory. A global mean wind speed of 6 $\mathrm{m\,s^{-1}}$ was chosen.

3. RESULTS

3.1 Ground Coverage

Fig. 1 shows the ground coverage for noon ascending and descending node orbits for a full day. The effects of the tilt strategy are apparent in Fig. 1 by the gap in equatorial coverage, where the tilt changes from $-20°$ (aft) to 20° (fore). The major differences are: 1) areas covered for a given day, 2) the angle the swaths make with respect to latitude, and 3) the local time of coverage. Regarding the latter point, ascending node orbits travel from afternoon in the South Pole through noon to morning in the North Pole, while descending node orbits travel from afternoon in the North Pole to morning in the South Pole. Thus descending node noon orbits will observe the Northern Hemisphere in the afternoon, as opposed to morning for ascending node. These local times encountered by the two nodes are shown in Fig. 2.

3.2 Zenith Angles at Equinox

The solar zenith angles encountered by ascending and descending nodes at the vernal equinox are identical (Fig. 3), as are spacecraft zenith angles (Fig. 4). Thus the path lengths of irradiance travelling through the atmosphere and into the ocean and the radiance travelling back to the spacecraft should be the same. The path length has important ramifications for radiative transfer in the atmospheric correction algorithms.

3.3 Azimuth Angles at Equinox

Solar azimuth angles encountered by ascending and descending nodes are substantially different (Fig. 5). The angles may be verified by analyzing the coverage plots (Fig. 1) and noting that for noon orbits at the equinox the sub-solar point is at the equator and along-track. The differences result from the different approaches to the equator taken by ascending and descending nodes. A difference plot is also shown in Fig. 5 for solar azimuth angle. Positive difference means that descending node produced a larger solar azimuth angle at a given point in the scan. Differences ranged from 0 to 360°. Note that these are not the smallest difference, i.e., a difference of 360° is really a difference of zero.

Differences are also apparent in spacecraft azimuth angle (Fig. 6), however, they are not as extreme. A difference plot (Fig. 6) shows that the ranges are between 0 and 120°. Differences in spacecraft azimuth are due to the difference in the angle made between the cross-track scan and latitude.

Despite large differences in solar and spacecraft azimuth angles, relative azimuth angles are remarkably similar for ascending and descending nodes (Fig. 7). A difference plot (Fig. 7) shows that the differences are between $-4°$ and 5°. This range also only occurs near the equator and most of the orbit contains negligible (less than 1°) differences. Note that for relative azimuth, the minimum angle between sun and spacecraft are shown, such that the maximum possible difference is 180°. Since it is the relative azimuth that is used in radiative transfer calculations and

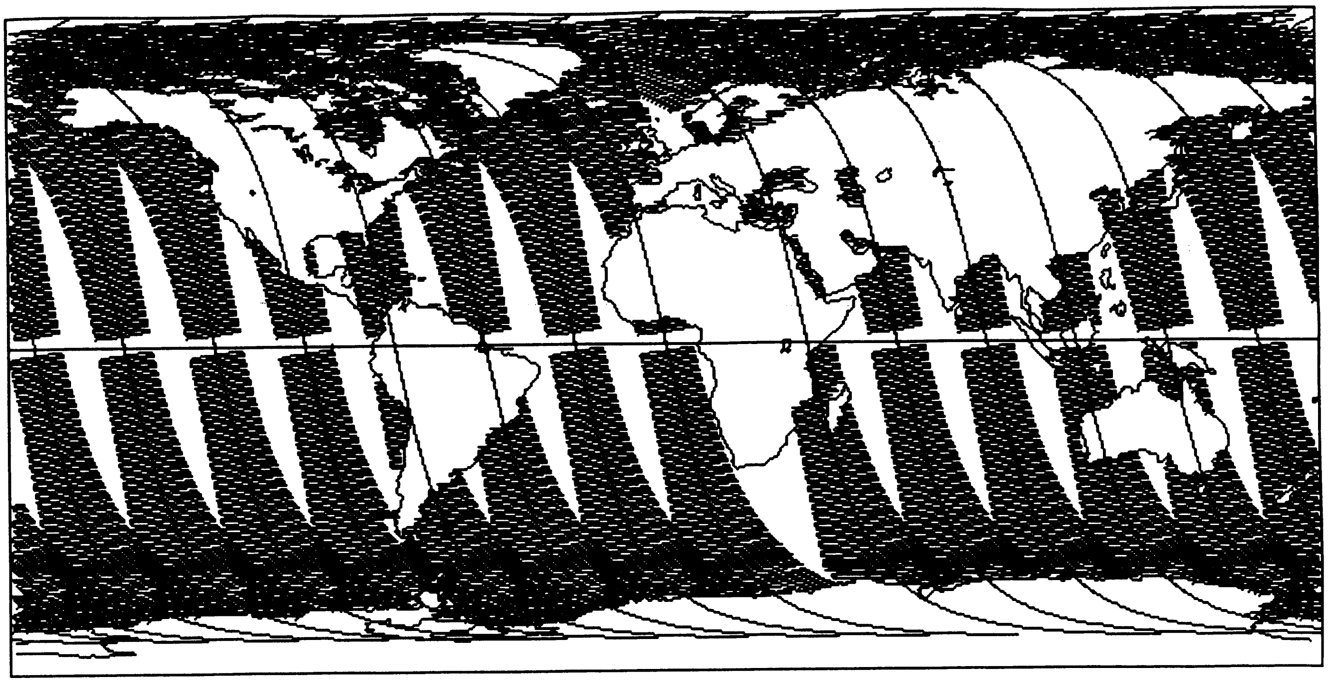

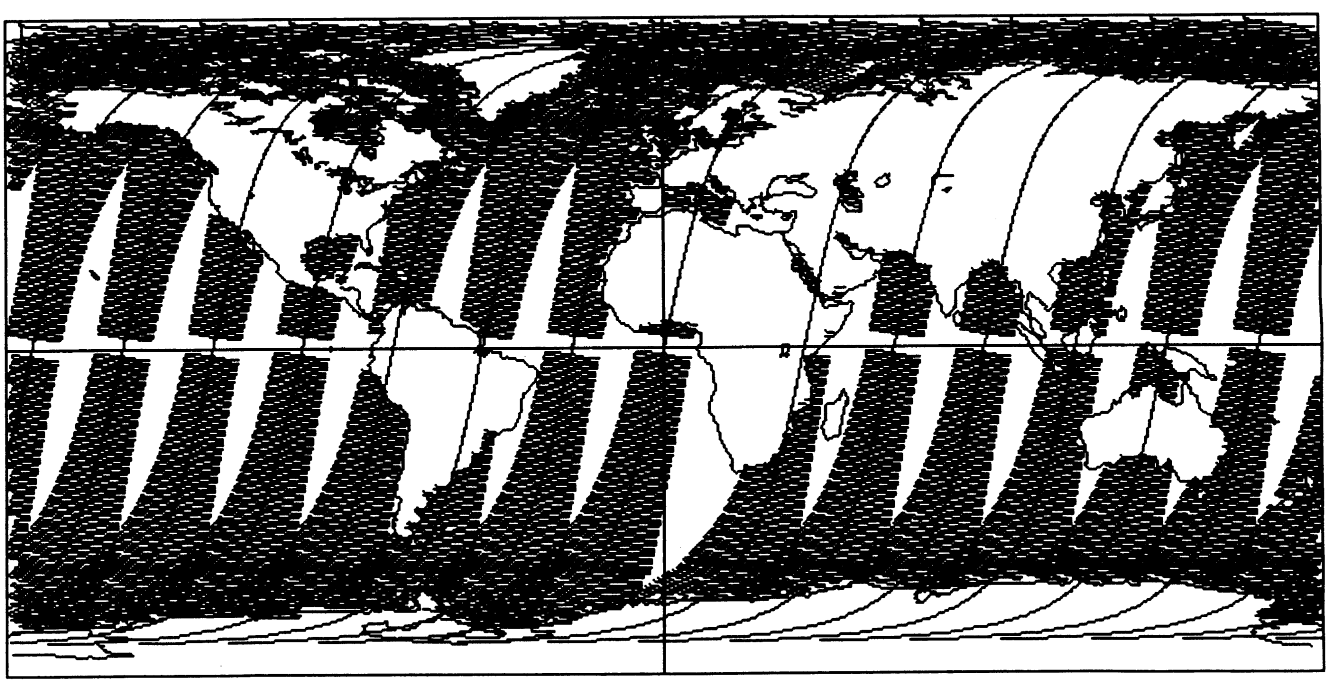

Fig. 1. a) Ground coverage of a SeaWiFS sensor in ascending node, with GAC coverage (scan of ±45°) for a full day. **b)** Descending node.

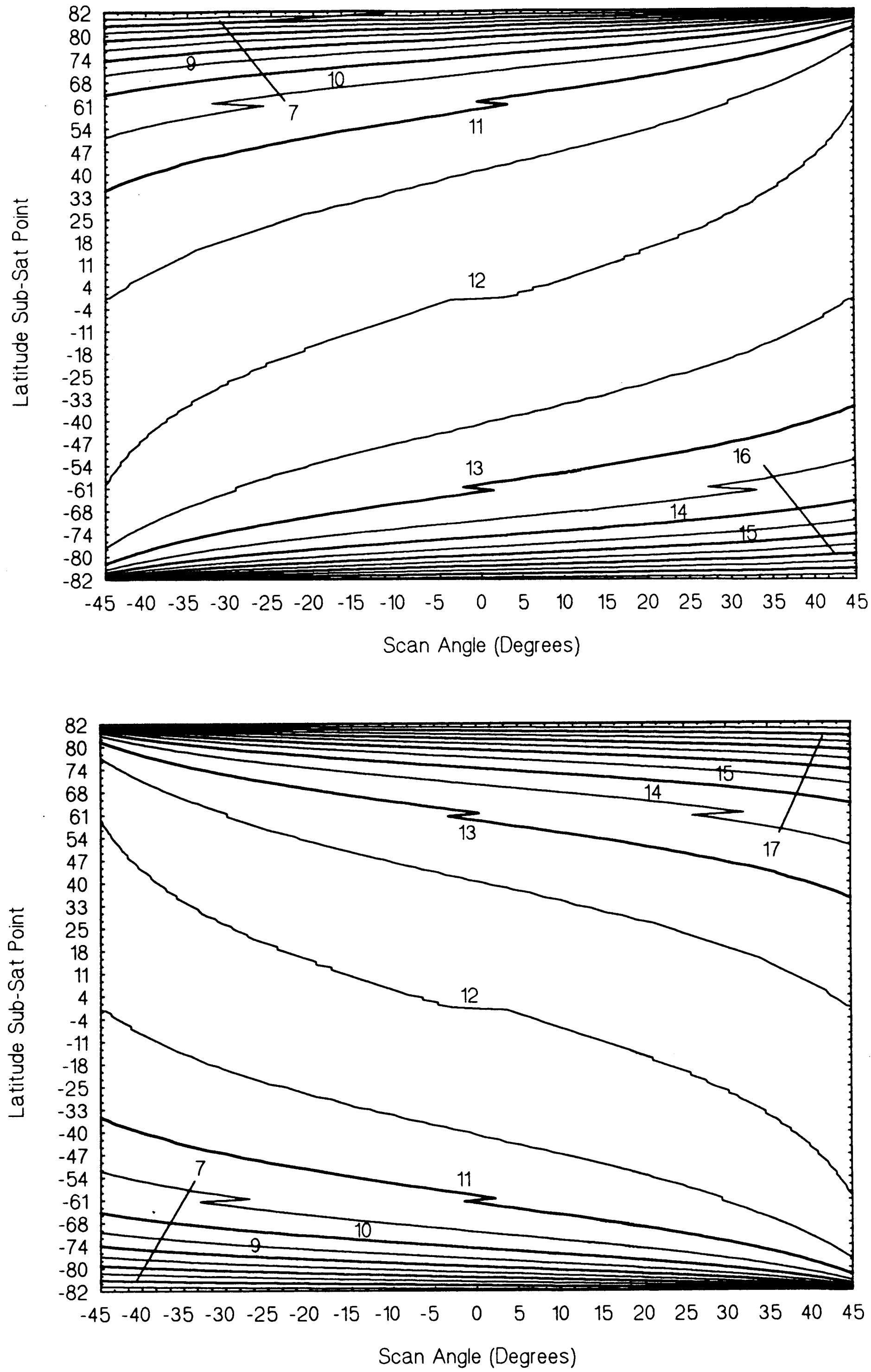

Fig. 2. Distribution of local time for ascending and descending noon orbits. The noon local time is only achieved at the equator. Note that the sub-satellite point is denoted on the ordinate, but that the actual location of the pixel in the scan is usually much different due to inclination and the tilting strategy. **a)** Ascending node. In ascending node the spacecraft travels from afternoon in the Southern Hemisphere to morning in the Northern Hemisphere. **b)** Descending node. In descending node the spacecraft travels from afternoon in the Northern Hemisphere to morning in the southern hemisphere.

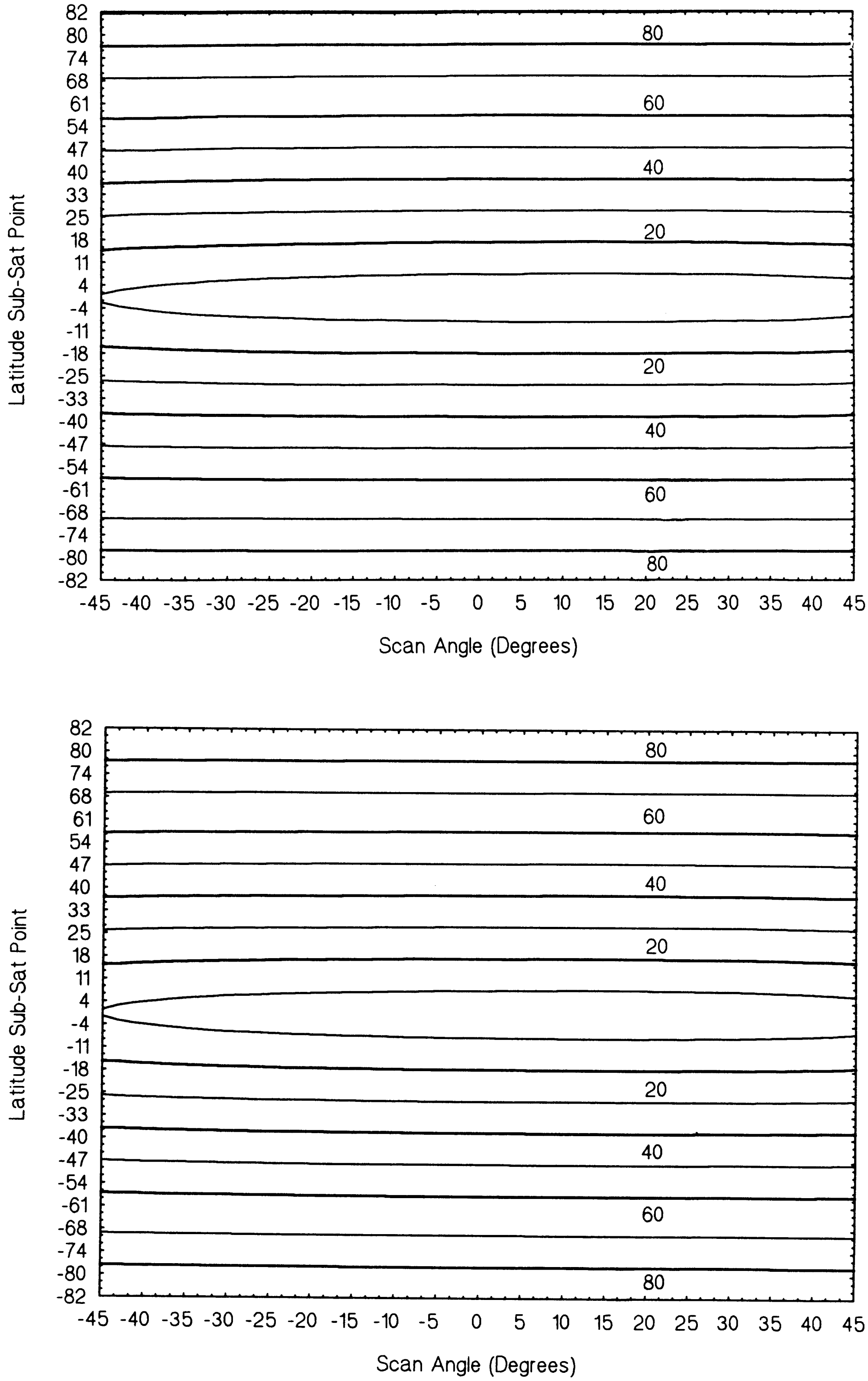

Fig. 3. a) Solar zenith angle distribution encountered for an ascending node, noon orbit, for the vernal equinox. **b)** Descending node.

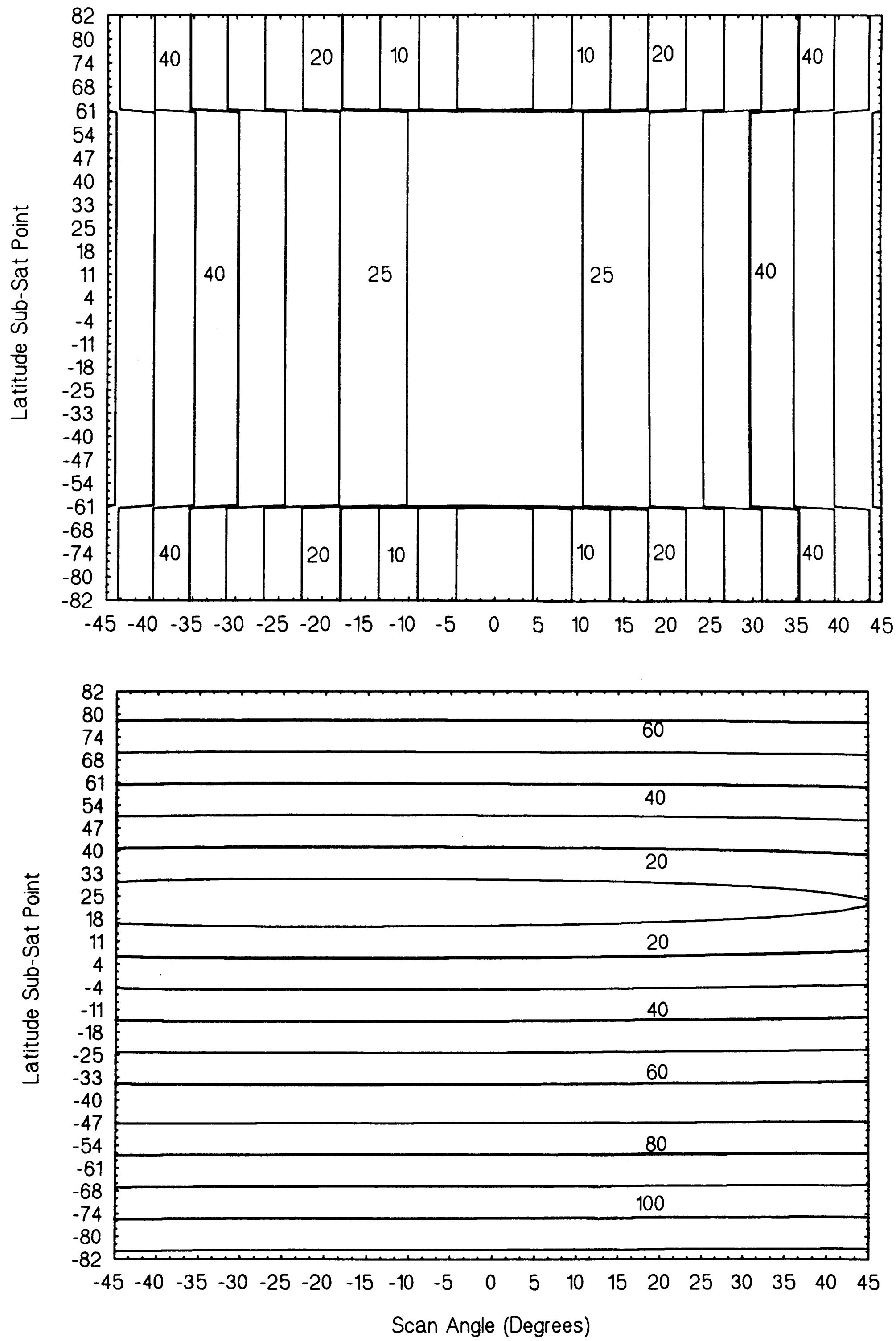

Fig. 4. Spacecraft zenith angles encountered by ascending and descending node orbits, for the vernal equinox. The tilting strategy is described in the text and may be noted in the figure by discontinuities at 60° N and S, where the tilt changes from nadir-pointing to ±20°. **a)** Ascending node. **b)** Descending node.

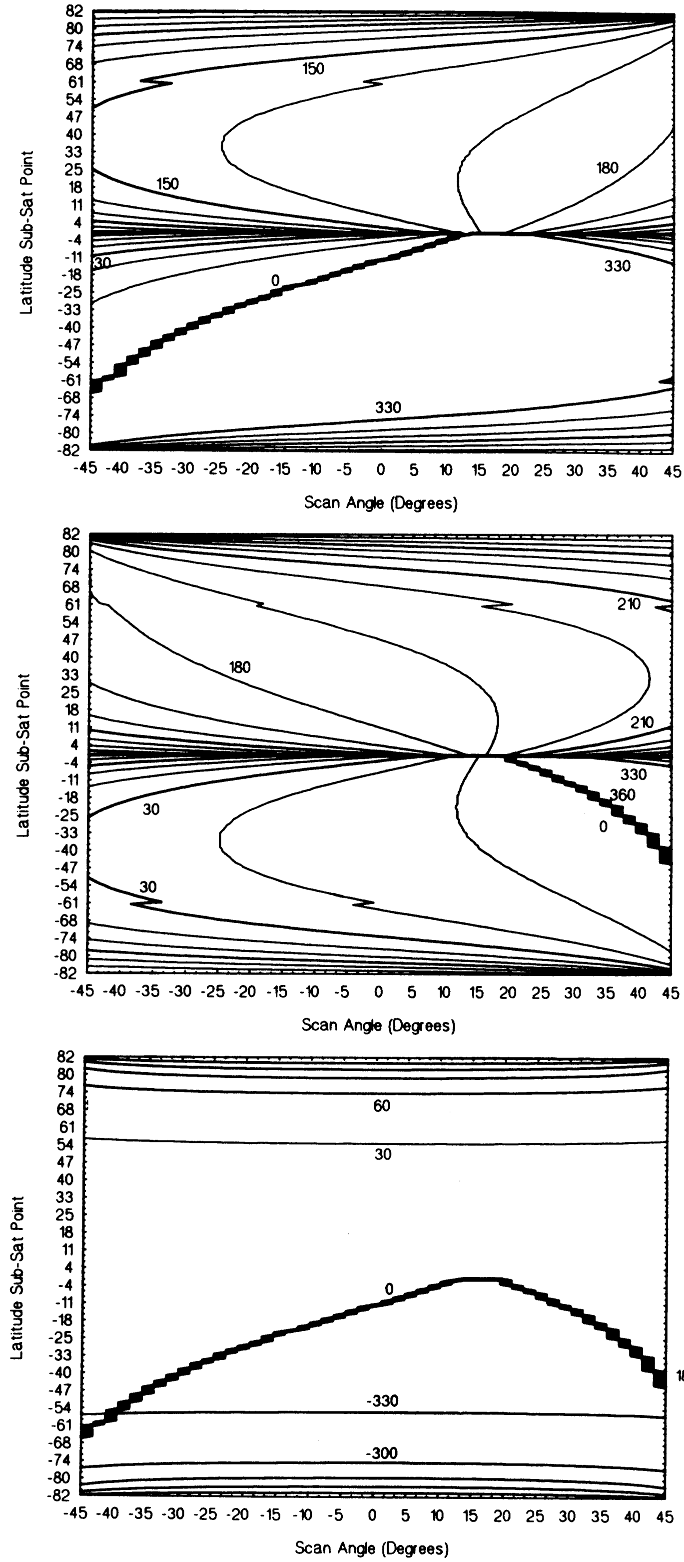

Fig. 5. a) Solar azimuth angle distribution encountered for an ascending node, noon orbit, for the vernal equinox. **b)** Descending node. **c)** Difference plot of solar azimuth angles for descending and ascending nodes. A positive difference indicates the descending node had a larger solar azimuth angle, while a negative difference indicates descending node had a smaller angle. Note these angles are not the smallest difference.

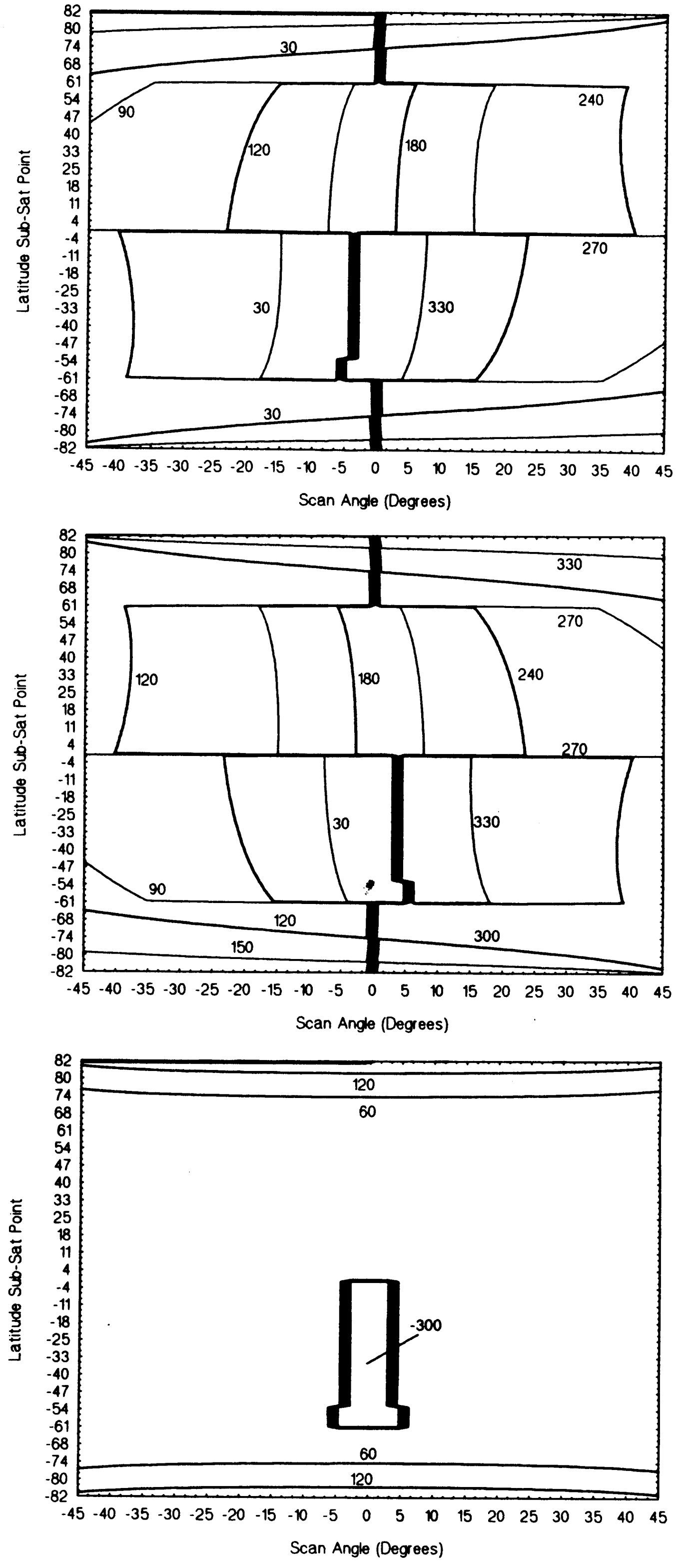

Fig. 6. a) Spacecraft azimuth angle distribution encountered for an ascending node, noon orbit, for the vernal equinox. **b)** Descending node. **c)** Difference plot of spacecraft azimuth angles for descending and ascending nodes. A positive difference indicates the descending node had a larger spacecraft azimuth angle, while a negative difference indicates descending node had a smaller angle. Note these angles are not the smallest difference.

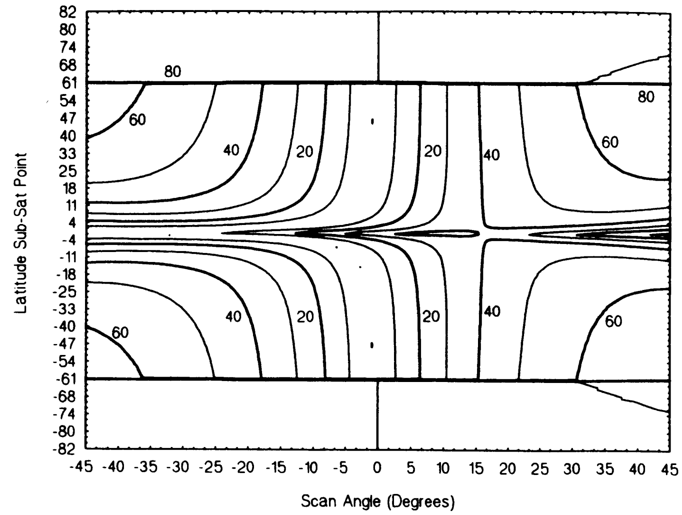

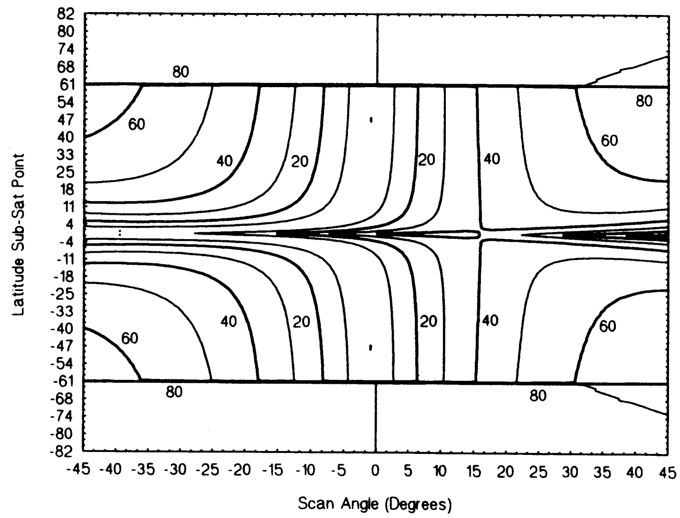

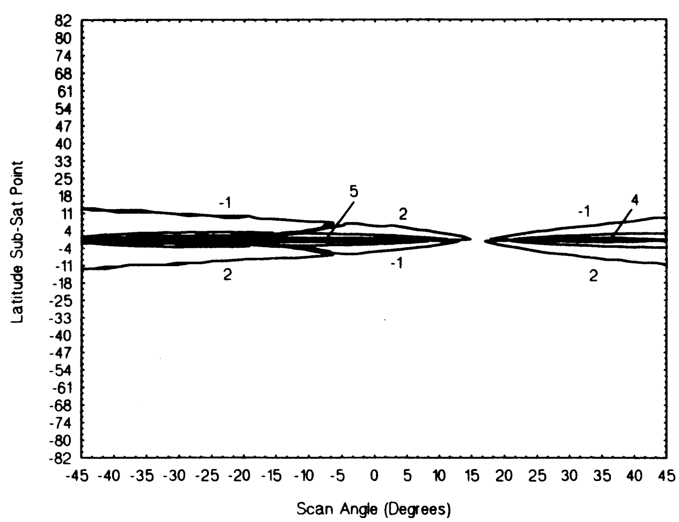

Fig. 7. a) Relative azimuth angle (angle between sun and spacecraft) distribution encountered for an ascending node, noon orbit, for the vernal equinox. **b)** Descending node. **c)** Difference plot of relative azimuth angles for descending and ascending nodes.

in the calculation of sun glint and not the solar and spacecraft azimuth angles individually, these plots show that there is little difference between ascending and descending nodes.

3.4 Sun Glint at Equinox

Sun glint radiance is a good indicator of the importance of solar and viewing geometries on radiative transfer for atmospheric correction and is also important in and of itself. This is because sun glint is determined by the solar and viewing geometries in a manner nearly identical to aerosol and Rayleigh scattering. Maximum sun glint occurs at the forward scattering area (where relative azimuth is 180°) and where solar and spacecraft zenith angles are identical. Maximum scattering also occurs in the forward direction for most aerosols. Sun glint at 500 nm was computed since this represents a spectral maximum. This wavelength is near the SeaWiFS 490 nm band.

As may be expected from the relative azimuth and zenith angle plots, there is an indistinguishable difference in sun glint between ascending and descending nodes (see Fig. 8). The maximum occurs near the equator, which is expected for the equinox. The small sun glint radiance near 60° N and 60° S is where the tilt changes from 0° to ±20°.

A sun glint difference plot more clearly shows the relative importance of ascending versus descending node (Fig. 8). While descending node obtains slightly higher sun glint just north of the equator, it obtains less below. Thus over the entire orbit there can be considered to be no difference. The absolute magnitude of the differences is small in any event, not exceeding approximately 0.1 mW cm^{-2} $\mu\mathrm{m}^{-1}$ sr^{-1}.

3.5 Zenith Angles at Solstice

The solar zenith angles encountered by ascending and descending nodes at the Northern Hemisphere summer solstice are different, but symmetrical (Fig. 9). On this day, an ascending orbit passes to the west of the sub-solar point, while a descending orbit passes to the east. Thus minimum solar zenith angles are obtained on the right (east) side of the ascending scan and on the left (west) side of the descending scan. Spacecraft zenith angles do not change substantially from the equinox case.

3.6 Azimuth Angles at Solstice

Only relative azimuth angles are shown for the solstice case, since they are the important parameter for atmospheric correction. Also, it is important to note that spacecraft azimuth angles do not change substantially as a function of node.

Unlike the equinox case, relative azimuth angles are quite different for ascending and descending orbits (Fig. 10). A difference plot (Fig. 10) shows that the angles are smaller for descending node, reaching −50°. This is an asymmetry due to the Equation of Time: the sub-solar point is not always exactly overhead at noon (Iqbal 1983). In fact, the sub-solar point is usually a small distance east or west of directly overhead at noon. For the summer solstice it is slightly east.

3.7 Sun Glint at Solstice

As might be expected from the difference in the solar zenith angles and relative azimuth angles in ascending and descending orbits at noon, sun glint radiance is also different (Fig. 11). The location of the maximum is shifted slightly east for ascending node and slightly west for descending node. This is a consequence of the fact that, at the solstice, the sub-solar point is located east of the ascending node sub-satellite track and west of the descending node.

Differences in sun glint are plotted in Fig. 11. The magnitude of the differences is relatively large—up to approximately 0.5 mW cm^{-2} $\mu\mathrm{m}^{-1}$ sr^{-1}. This has important consequences for ocean observations and atmospheric correction. However, the differences are symmetrical. An increase in sun glint on the western part of the scan for descending orbits is compensated by a reduction on the eastern part. Thus, taken as an entire orbit, there appears to be no loss of quality of ocean observations by descending node.

3.8 Importance of Equator Crossing Time

To evaluate the importance of deviations from a noon equator crossing time (ECT), a one year simulation was performed, which also diminishes the importance of the Equation of Time. ECTs of noon ±1.5 hours were assessed, for both ascending and descending orbits. At the outset it must be emphasized that exact noon ECTs provide the minimum mean solar zenith angle for both Northern and Southern Hemispheres.

For ascending node, lowest mean solar zenith angles are obtained in the Northern Hemisphere for 12:30 ECT and in the Southern Hemisphere for an 11:30 ECT (Fig. 12). The worst (largest) solar zenith angles are obtained for a 10:30 ECT in the Northern Hemisphere and a 1:30 ECT in the Southern. Maximum departures occurred near the equator and amounted to approximately 10°. Generally, morning orbits are preferred to obtain smaller zenith angles in the Southern Hemisphere and afternoon orbits for the Northern Hemisphere.

For descending node, lowest mean solar zenith angles are obtained for 11:30 ECT in the Northern Hemisphere and 12:30 ECT in the southern (Fig. 12). The largest angles are obtained for a 1:30 ECT in the northern hemisphere and a 10:30 ECT in the Southern. Again the maximum departure is approximately 10°. In contrast to ascending orbits, afternoon orbits are preferred for the Southern Hemisphere and morning for the Northern Hemisphere

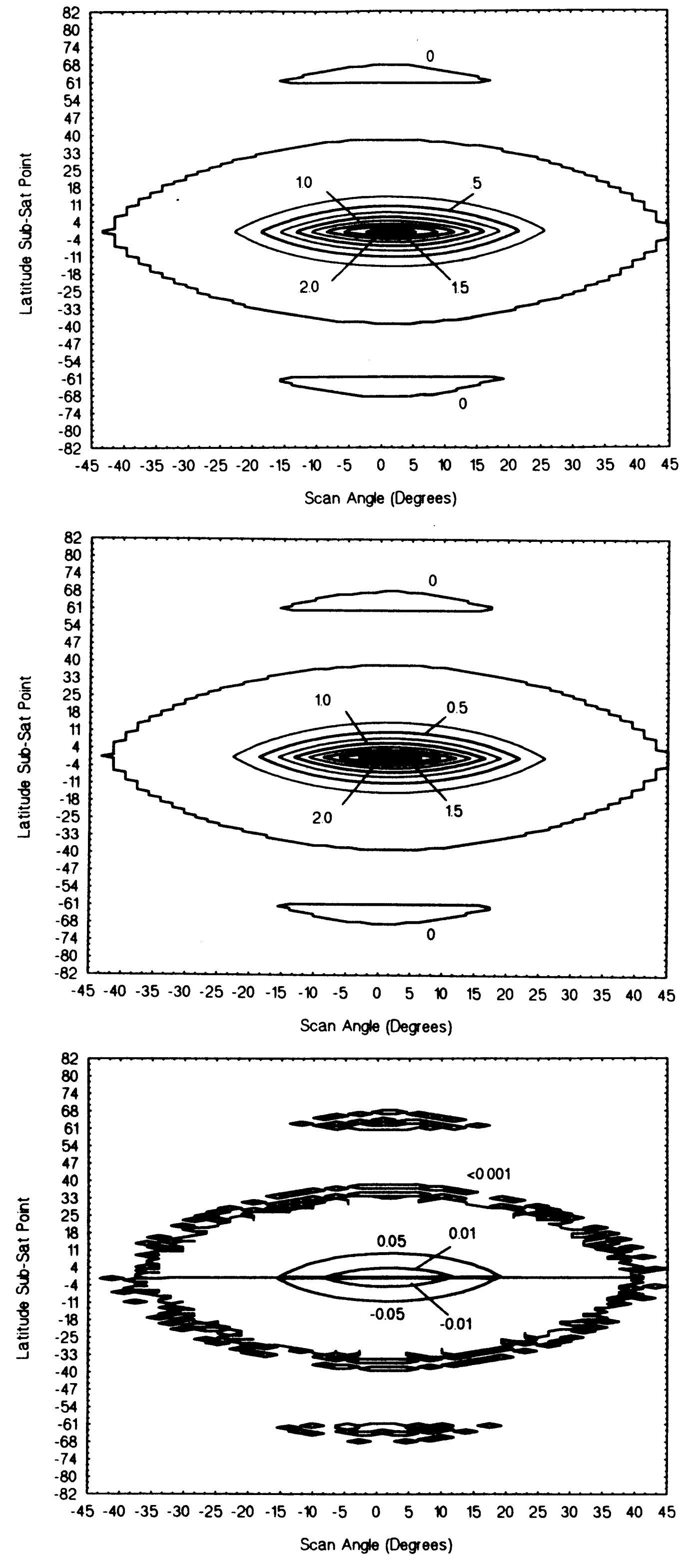

Fig. 8. a) Relative azimuth angle (angle between sun and spacecraft) distribution encountered for an ascending node, noon orbit, for the vernal equinox. **b)** Descending node. **c)** Difference plot of relative azimuth angles for descending and ascending nodes.

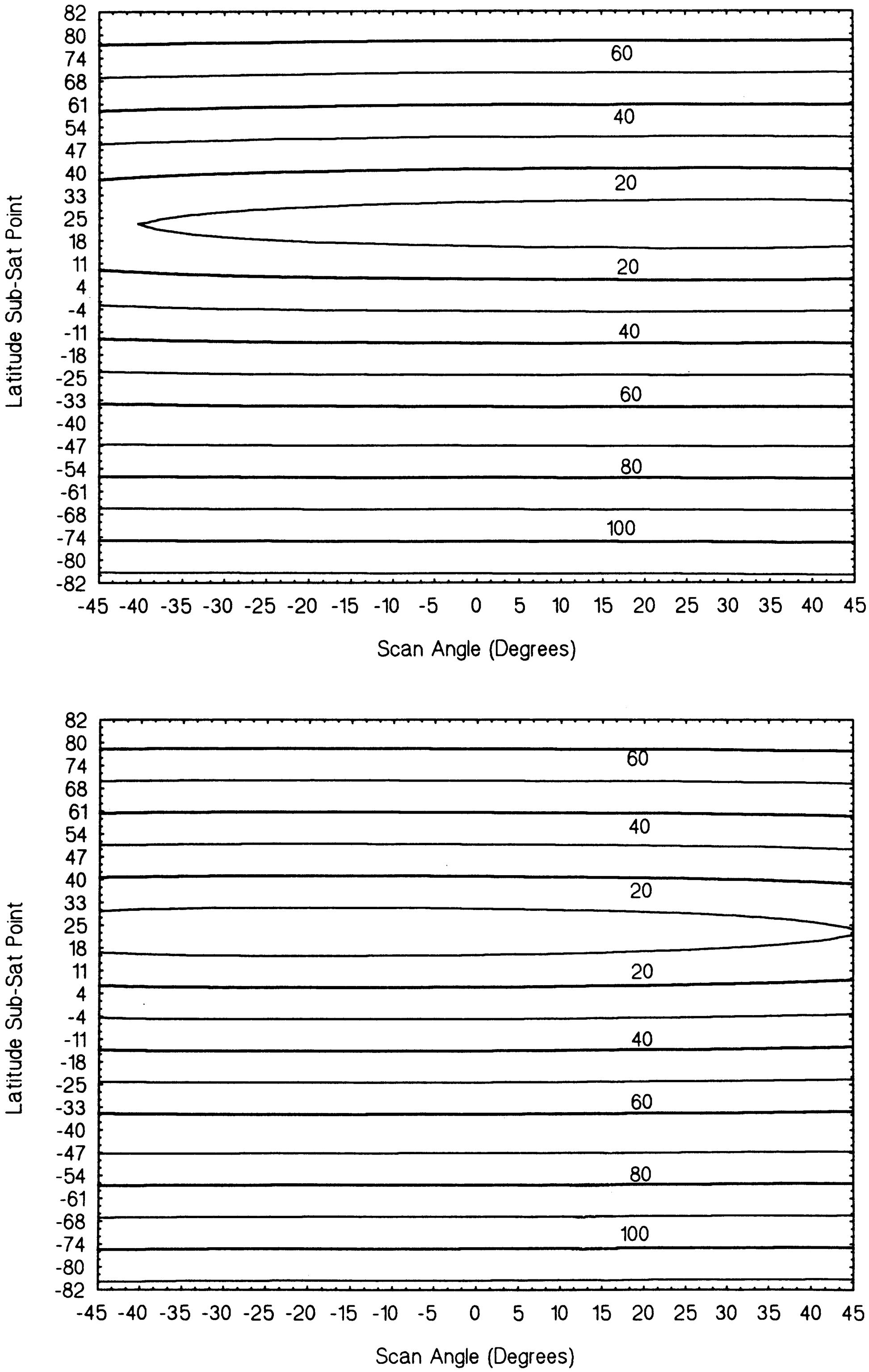

Fig. 9. a) Solar zenith angle distribution encountered for an ascending node, noon orbit, for the Northern Hemisphere summer solstice. The smallest angles are located to the east because in ascending node the sub-satellite track crosses the sub-solar point to the west. **b)** Descending node. The smallest angles are located to the west because in ascending node the sub-satellite track crosses the sub-solar point to the east.

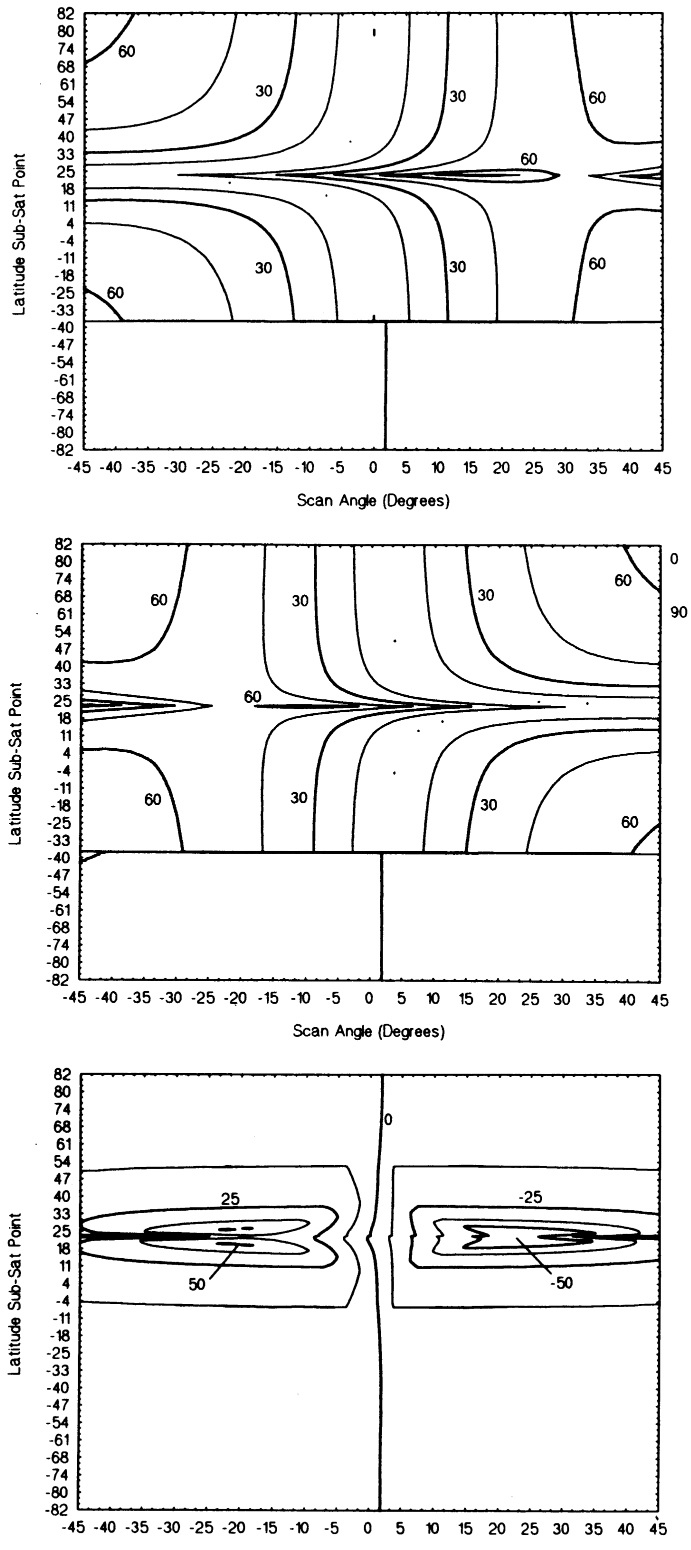

Fig. 10. a) Relative azimuth angle distribution encountered for an ascending node, noon orbit, for the Northern Hemisphere summer solstice. **b)** Descending node. **c)** Difference plot of relative azimuth angles for descending and ascending nodes.

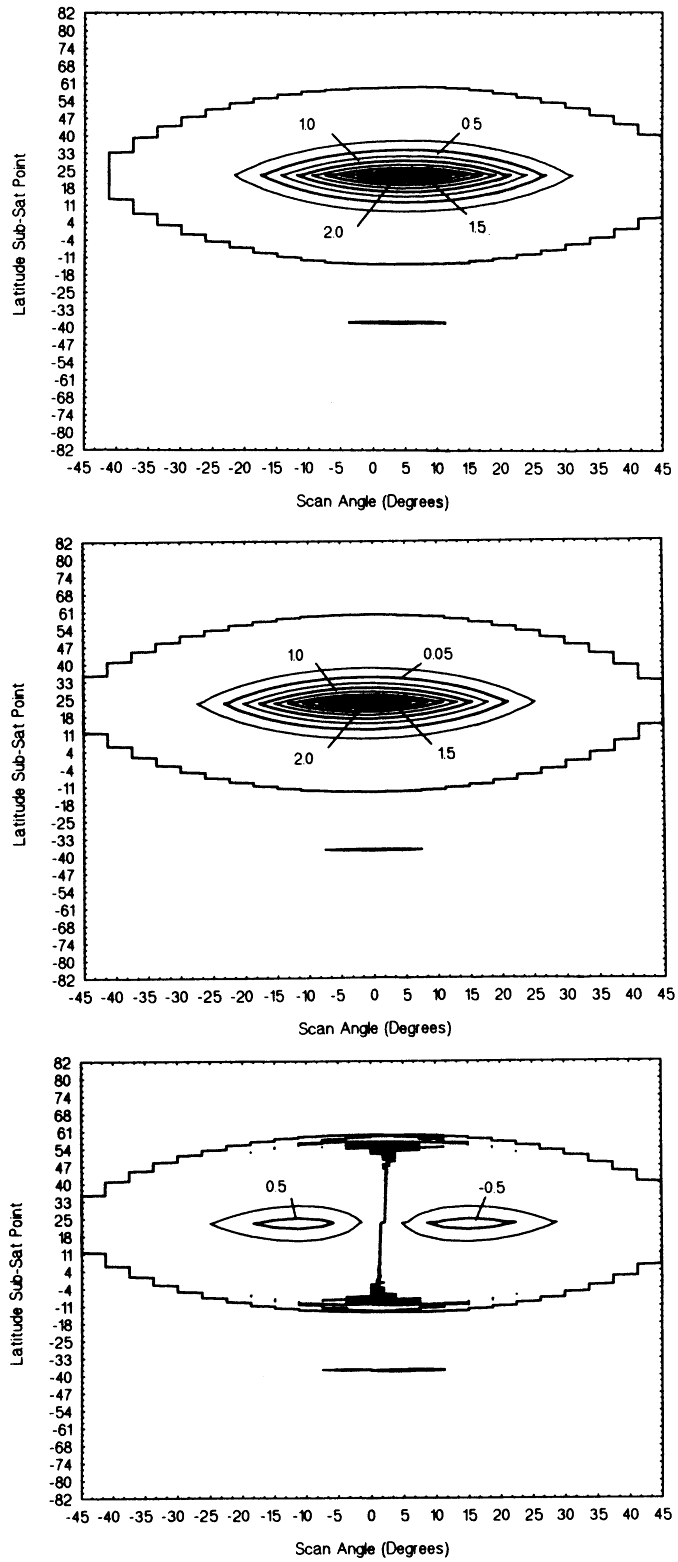

Fig. 11. a) Sun glint radiance distribution at 500 nm encountered for an ascending node, noon orbit, for the Northern Hemisphere summer solstice. **b)** Descending node. **c)** Difference plot of sun glint radiance for descending and ascending nodes.

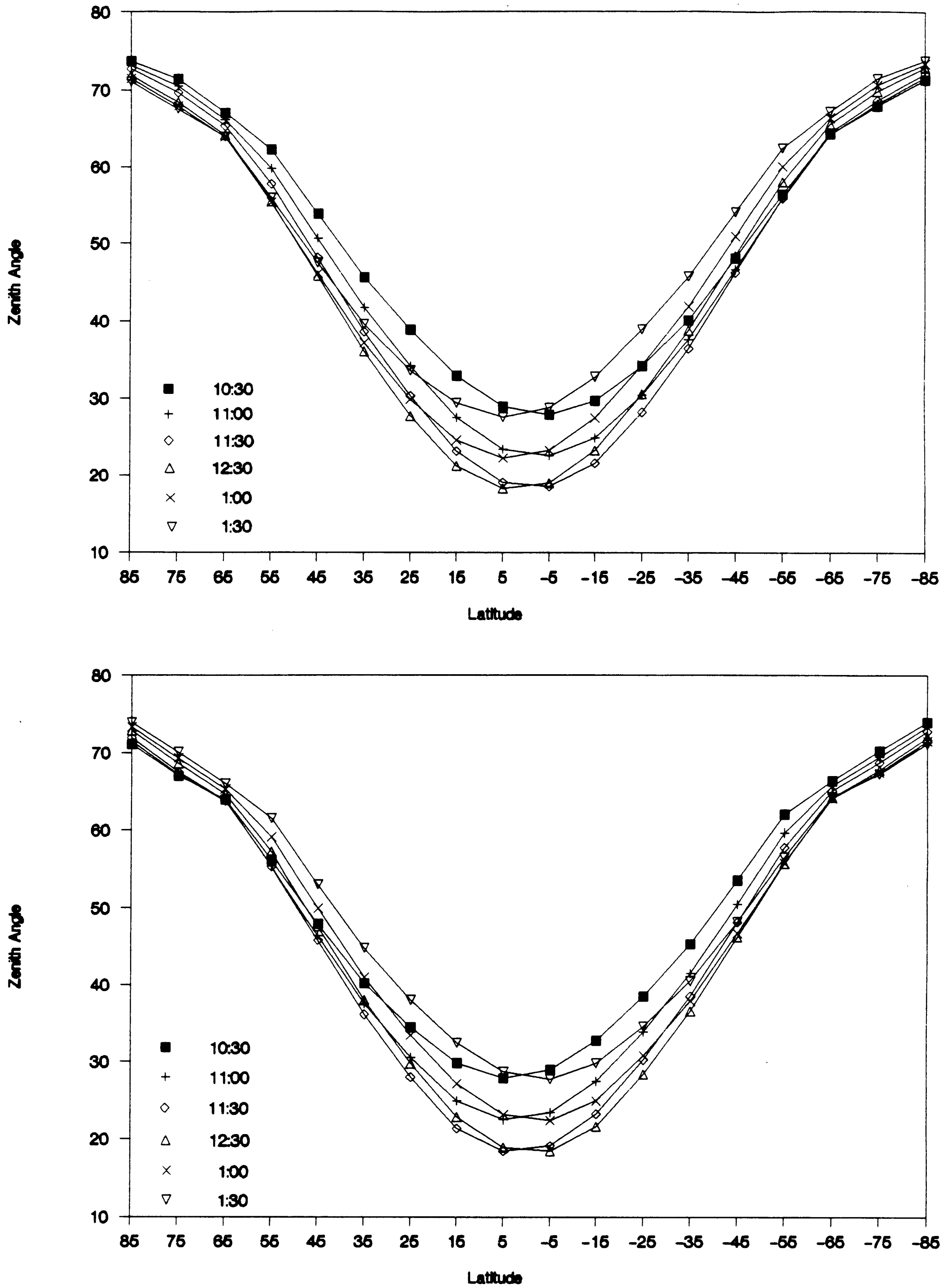

Fig. 12. a) Mean solar zenith angles encountered for ascending nodes at different equator crossing times. This analysis was performed for an entire year to minimize the effect of the Equation of Time. The smallest solar zenith angles are obtained in the Northern Hemisphere for afternoon ascending orbits, while the smallest angles are obtained in the Southern Hemisphere for morning ascending orbits. **b)** Descending node. The smallest solar zenith angles are obtained in the Northern Hemisphere for morning descending orbits, while the smallest angles are obtained in the Southern Hemisphere for afternoon descending orbits.

for descending orbits. These conclusions are summarized in Table 3.

Table 3. Lowest mean solar zenith angles for ascending and descending node orbits.

Hemisphere	Ascending Node	Descending Node
Northern	Afternoon	Morning
Southern	Morning	Afternoon

4. DISCUSSION

Simulations of the solar and viewing geometries encountered by noon ascending and descending node orbits revealed substantial differences in solar azimuth and spacecraft azimuth angles both at equinox and at the Northern Hemisphere summer solstice. Negligible differences in solar and spacecraft zenith angles, relative azimuth angles and sun glint were obtained at the equinox. However, large differences were found in solar zenith angles, relative azimuths and sun glint for the solstice. These differences evened out across the scan, however, an increase in sun glint in descending node over that in ascending node on the western part of the scan was compensated by a decrease on the eastern part of the scan. Thus, no advantage or disadvantage could be conferred upon either ascending or descending node for noon orbits.

Differences occurred for ascending and descending node orbits that deviated from a noon equator crossing time. To obtain the lowest mean solar zenith angles, afternoon orbits are preferred for ascending node in the Northern Hemisphere and morning for the Southern Hemisphere. Concerning the descending node, morning orbits are preferred for the Northern Hemisphere, and afternoon for the Southern Hemisphere.

Glossary

CZCS Coastal Zone Color Scanner
ECT Equator Crossing Time
GAC Global Area Coverage
IFOV Instantaneous Field-Of-View
SeaWiFS Sea-viewing Wide Field-of-view Sensor

References

Cox, C., and W. Munk, 1954: Measurement of the roughness of the sea surface from photographs of the sun's glitter. *J. Mar. Res.*, **44,** 838-850.

Iqbal, M., 1983: *An Introduction to Solar Radiation.* Academic Press, 390 pp.

Wilson, W.H., R.C. Smith, and J.W. Nolten, 1981: The CZCS geolocation algorithms. *SIO Ref. 81-32,* Scripps Institute of Oceanography, 37 pp.

REPORT DOCUMENTATION PAGE

Form Approved
OMB No. 0704-0188

1. AGENCY USE ONLY *(Leave blank)*	2. REPORT DATE	3. REPORT TYPE AND DATES COVERED
	September 1992	Technical Memorandum

4. TITLE AND SUBTITLE
SeaWiFS Technical Report Series
Volume 2–An Analysis of Orbit Selection for SeaWiFS: Ascending vs. Descending Node

5. FUNDING NUMBERS
Code 970.2

6. AUTHOR(S)
Watson W. Gregg

Series Editors: Stanford B. Hooker and Elaine R. Firestone

7. PERFORMING ORGANIZATION NAME(S) AND ADDRESS(ES)
Laboratory for Hydrospheric Processes
Goddard Space Flight Center
Greenbelt, Maryland 20771

8. PERFORMING ORGANIZATION REPORT NUMBER
92B00122

9. SPONSORING/MONITORING AGENCY NAME(S) AND ADDRESS(ES)
National Aeronautics and Space Administration
Washington, D.C. 20546–0001

10. SPONSORING/MONITORING AGENCY REPORT NUMBER
TM–104566, Vol. 2

11. SUPPLEMENTARY NOTES
Elaine R. Firestone: General Sciences Corporation, Laurel, Maryland.

12a. DISTRIBUTION/AVAILABILITY STATEMENT
Unclassified–Unlimited
Subject Category 48

12b. DISTRIBUTION CODE

13. ABSTRACT *(Maximum 200 words)*

Due to range safety considerations, the Sea-viewing Wide Field-of-view Sensor (SeaWiFS) ocean color instrument may be required to be launched into a near-noon descending node, as opposed to the ascending node used by the predecessor sensor, the Coastal Zone Color Scanner (CZCS). The relative importance of ascending versus descending near-noon orbits was assessed here to determine if descending node will meet the scientific requirements of SeaWiFS. Analyses focused on ground coverage, local times of coverage, solar and viewing geometries (zenith and azimuth angles), and sun glint. Differences were found in the areas covered by individual orbits, but were not important when taken over a 16 day repeat time. Local time of coverage was also different: for ascending node orbits the Northern Hemisphere was observed in the morning and the Southern Hemisphere in the afternoon, while for descending node orbits the Northern Hemisphere was observed in the afternoon and the Southern in the morning. There were substantial differences in solar azimuth and spacecraft azimuth angles both at equinox and at the Northern Hemisphere summer solstice. Negligible differences in solar and spacecraft zenith angles, relative azimuth angles, and sun glint were obtained at the equinox. However, large differences were found in solar zenith angles, relative azimuths and sun glint for the solstice. These differences appeared to compensate across the scan, however, an increase in sun glint in descending node over that in ascending node on the western part of the scan was compensated by a decrease on the eastern part of the scan. Thus, no advantage or disadvantage could be conferred upon either ascending node o descending node for noon orbits. Analyses were also performed for ascending and descending node orbits that deviated from a noon equator crossing time. For ascending node, afternoon orbits produced the lowest mean solar zenith angles in the Northern Hemisphere; and morning orbits produced the lowest angles for the Southern Hemisphere. For descending node, morning orbits produced the lowest mean solar zenith angles for the Northern Hemisphere; afternoon orbits produced the lowest angles for the Southern Hemisphere.

14. SUBJECT TERMS
Oceanography, SeaWiFS, Descending Node, Ascending Node, Orbit, Viewing Geometry, Zenith, Azimuth, SeaStar, Sun Glint, Equator Crossing Time, Solstice, Equinox

15. NUMBER OF PAGES
18

16. PRICE CODE

17. SECURITY CLASSIFICATION OF REPORT	18. SECURITY CLASSIFICATION OF THIS PAGE	19. SECURITY CLASSIFICATION OF ABSTRACT	20. LIMITATION OF ABSTRACT
Unclassified	Unclassified	Unclassified	Unlimited